**INTERNATIONAL JOURNAL OF OPTIMIZATION IN CIVIL ENGINEERING**
***Int. J. Optim. Civil Eng., 2017; 7(2):269-290***

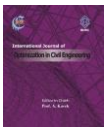



# SIMULTANOUS OPTIMIZATION OF SIZE AND CONNECTION ARRANGEMENT FOR LOW-RISE STEEL PLATE SHEAR WALL SYSTEMS

P. Mohebian[1], M. Mousavi[1] and H. Rahami[2*, †]
[1]*Department of Civil Engineering, Faculty of Engineering, Arak University, Iran*
[2]*School of Engineering Science, College of Engineering, University of Tehran, Tehran, Iran*

## ABSTRACT

The present study is concerned with the simultaneous optimization of the size of components and the arrangement of connections for performance-based seismic design of low-rise SPSWs. Design variables include the size of beams and columns, the thickness of the infill panels, the type of each beam-to-column connection and the type of each infill-to-boundary frame connection. The objective function is considered to be the sum of the material cost and rigid connection fabrication cost. For comparison purposes, the SPSW model is also optimized with regard to two fixed connection arrangements. To fulfill the optimization task a new hybrid optimization algorithm called CBO-Jaya is proposed. The performance of the proposed hybrid optimization algorithm is assessed by two benchmark optimization problems. The results of the application of the proposed algorithm to the benchmark problem indicate the efficiency, robustness, and the fast convergence of the proposed algorithm compared with other meta-heuristic algorithms. The achieved results for the SPSWs demonstrate that incorporating the optimal arrangement of beam-to-column and infill-to-boundary frame connections into the optimization procedure results in considerable reduction of the overall cost.

**Keywords:** steel plate shear wall; a hybrid CBO-Jaya algorithm; optimal performance-based seismic design; connection arrangement.

Received: 12 September 2016; Accepted: 17 November 2016

[*]Corresponding author: School of Engineering Science, College of Engineering, University of Tehran, Tehran, Iran
[†]E-mail address: hrahami@ut.ac.ir (H. Rahami)

## 1. INTRODUCTION

In recent decades, steel plate shear walls (SPSWs) have been greatly regarded by both researchers and practicing engineers as an efficient lateral load resisting system. In a typical application of a SPSW, un-stiffened infill panels are connected to the surrounding beams and columns, which are called horizontal boundary elements (HBEs) and vertical boundary elements (VBEs), respectively. SPSWs provide high seismic performance and offer praiseworthy characteristics such as substantial strength and stiffness, significant ductility, considerable energy absorption capability, and ease of construction [1,2]. However, the conventional SPSW configuration imposes significant force demands on boundary elements, which consequently leads to an uneconomic design [3]. Several alternative methods have been suggested to resolve this problem. In this regard, the analytical study implemented by Xue and Lu [4] could be considered as one of the first attempts focused on this issue. Based on the results of the finite element analysis carried out for four three-bay, twelve-story frames including rigid beam-to-column connections in their adjacent bays and steel panels located in their middle bay, it was concluded that the use of simple connections in the middle bay and connecting the infill panels only to HBEs are accompanied by a reduction in demands on VBEs. As another approaches, it can be referred to light-gauge and low yield point steel plate shear walls [5,6], restrained SPSW which is comprised of pin-ended horizontal struts along the height of each story [7] and perforated steel plate shear walls with reduced beam section (RBS) connections [8].

Among all the promising approaches mentioned above, however there is a challenging area with the Xue and Lu's investigation [4]. Because only a limited number of cases were participated in the analysis, their result may not be categorically reliable in general [9]. On the other hand the contributions of the deformation capacity of elements were not taken into account [10]. Apart from that study, no more attention has been paid to expand the knowledge about the SPSW with regard to simultaneous use of simple and rigid beam-to-column connections together with partially and fully connected web plates. Hence there remains a need for further research regarding the methodology. The attempt to attain the most desirable connection arrangement for a given SPSW in a cost-effective manner raises an optimization problem. This paper deals with the optimal seismic design of low-rise SPSW system in a way that the size of components as well as the arrangement of beam-to-column and infill-to-boundary frame connections are simultaneously considered as design variables and the overall cost of the structure are minimized subject to certain design constraints. In this optimization problem, some care is needed to obtain the solution that is acceptable from both practical and theoretical points of view. First, that in the present problem, the type of each beam-to-column connection can be varied as simple or rigid during the optimization process. It is clearly obvious that the fabrication cost of the rigid connections is much higher than simple ones due to their complex practical detailing [11]. This implies that the objective function must be representative of a cost minimization problem where both of material cost and rigid connection fabrication cost are taken into account. Second matter is concerned with choosing the right method for seismic analysis and design of the present SPSW optimization. Current seismic design codes require the capacity design principle for design of SPSWs. However, the force reduction factor (R-factor), which plays a key role in such a force-based design approach is only consistent with the

conventional SPSW configuration. Hence, the present work is implemented in the context of performance based seismic design with the employment of nonlinear static pushover analysis, which also captures the inelastic response of the structure.

Over the last decades, extensive studies have been accomplished in the field of the structural optimization. Along these lines, Kaveh and Farhoudi [12] performed the layout optimization of dual system of moment frame by utilizing GA, ACO, PSO and BB–BC algorithms. Gholizadeh and Shahrezaei [13] applied bat algorithm to find the optimal location of steel plate shear walls based on static equivalent lateral force design. In the sense of optimum performance based seismic design of steel moment frame, several researches have been carried out by making use of meta-heuristic algorithms, which can be referred to [14] and [15] as examples. By contrast to these referred studies, which were concentrated on the weight minimization, Kripakaran et al. [11] can be considered as the pioneers in the cost optimization of the steel moment frame with regard to the both of material and rigid connection costs. They used a series of GA algorithm to find the optimal location of a predefined number of rigid joints, and fed results into a heuristic algorithm to optimize the size of elements. On the other hand, recently Alberdi et al. [16] demonstrated the efficiency of meta-heuristic algorithms in connection topology optimization for steel moment frames. In these two later studies, because the aim was to design the steel moment frames against the wind load, the linear static analysis was easily utilized. The use of nonlinear static pushover analysis in the present optimization problem makes its process so time consuming and hence the need for an effective optimization algorithm is felt more than ever. Colliding Bodies Optimization (CBO) that has been developed by Kaveh and Mahdavi [17] is a powerful meta-heuristic optimization algorithm. The CBO algorithm is one of a few meta-heuristic optimization algorithms that is independent of any parameters controlling. However, regardless of the unique features of the CBO algorithm, its exploitation ability is week, which results in a slow convergence ratio and imposes computational costs [18]. Jaya algorithm is another impressive and parameter-less meta-heuristic algorithm that has been recently proposed by Rao [19]. In this paper, in order to overcome such a drawback involved in the CBO algorithm, a hybrid CBO-Jaya algorithm is presented. The CBO-Jaya algorithm contains the main structure of the CBO algorithm, in which some components of the Jaya algorithm is embedded with the intention of reinforcing the mechanism of the algorithm. Firstly, the performance of the proposed hybrid optimization algorithm is assessed by two benchmark optimization problems and then it will be used for simultaneous optimization of the size of components and the arrangement of connections for a low-rise SPSW.

## 2. PERFORMANCE BASED SEISMIC DESIGN

The performance-based seismic design (PBSD) procedure can be summarized into three steps. First, a performance objective, which couples a performance level with a given hazard level is selected. In this paper, the basic safety objective (BSO) is taken into consideration based upon ASCE-41 [20]. BSO stipulates that the structure should satisfy the life safety performance level (LS) as well as the collapse prevention performance level (CP) subject to hazard levels related to the ground motion with 10% and 2% possibility of occurrence in 50 years, respectively. In the second step, the seismic demands of the structure are determined

in terms of both force and deformation regarding to the hazard level. To perform this task, a nonlinear static pushover analysis is employed and the seismic demands are taken from the response of the structure at the target displacement i.e. the maximum roof displacement experienced by the structure during the seismic event. The target displacement is obtained via a trial and error procedure. The pseudo-code of this procedure can be found in [21]. The estimated target displacement is accounted by the following expression [20]:

$$\delta_t = C_0 C_1 C_2 S_a \frac{T_e^2}{4\pi^2} g, \tag{1}$$

where $C_0$ is an adjustment factor turning the spectral displacement of a SDOF system to a multi degree of freedom (MDOF) system roof displacement, $C_1$ is a modification factor that correlates the maximum expected inelastic displacements to the elastic displacements, $C_2$ stands for the impact of the pinched hysteretic shape on the maximum displacement response, $S_a$ is the response spectrum acceleration, $T_e$ is the effective fundamental period of the structure, which depends on the elastic fundamental period of the structure obtained by elastic dynamic analysis and $g$ is the acceleration of gravity.

Finally, the structural performance is assessed by comparing the estimated seismic demands against the acceptance criteria. Currently, ASCE-41 [20] does not cover the acceptance criteria for un-stiffened SPSWs. Hence, in the present study, the acceptance criteria of the steel moment frame given by ASCE-41 [20] are adopted for the seismic performance assessment of the frame members. Previously, Moghimi and Driver [22] also utilized the steel moment frame acceptance criteria to determine the column demands of a perforated SPSW. Moreover, here, the maximum infill panel deformation is defined in accordance with the result obtained by Berman [23], who evaluated the performance of the code designed SPSW by means of nonlinear response history analysis. As can be found in [23], the maximum infill panel ductility demands of a low-rise SPSW for the 10/50 and 2/50 hazard levels are about 6 and 12, respectively. Accordingly, for the SPSW considered here, these values are utilized as the acceptance criteria for the infill panel deformations at the LS and CP performance levels, respectively.

## 3. STATEMENT OF THE OPTIMIZATION PROBLEM

In the following sub-sections, the formulation characteristics of the present optimization problem are described.

### *3.1 Design variables*

The optimization problem of the present study contains four kinds of design variables: the size of frame members (E) including beams and columns, the thickness of the infill panels (F), the type of each beam-to-column connection (G) as either simple or rigid, and the type of each infill-to-boundary frame connection (H) as either full or partial. The vector of design variables is as follows:

$$\mathrm{X} = [\mathrm{E}, \mathrm{F}, \mathrm{G}, \mathrm{H}] \tag{2a}$$

$$K = [K_1, K_2, \dots, K_i, \dots, K_{nK}], \quad where\ K = E, F, G, H \tag{2b}$$

where $K_i$ and $nK$ represent the $i$th group and the total number of groups for design variables of type $K$, respectively.

*3.2 Objective function*

The principal purpose of the present formulation is to seek the best form of the structure including the material distributions and the connection arrangements in such a way that the total cost of the structure is minimized. According to [11] and [16] the contributions of the material cost as well as rigid connection fabrication cost are taken into account. The cost function of the present optimization problem is as follows:

$$f_{cost}(X) = \sum_{i=1}^{nE} A_i \sum_{j=1}^{nm} \rho_j L_j + \sum_{i=1}^{nF} t_{w,i} \sum_{j=1}^{np} \rho_j L_{HBE,j}\, h_{VBE,j} + \frac{C_r}{C_s}.N_R \tag{3}$$

where $A_i$ indicates the cross-sectional area for the group $i$ of the frame member design variables, $\rho_j$ and $L_j$ represent the material mass density and the length of the $j$th frame member, $nm$ is the total number of frame members, $t_{w,i}$ denotes the infill panel thickness for the group $i$ of the infill panel design variables, $L_{HBE,j}$ refers to the length of the $j$th HBE and $h_{VBE,j}$ is the height of the $j$th VBE, $np$ is the number of infill panels, $N_R$ implies the total number of rigid beam-to-column connections, $C_s$ is the unit cost of steel material per metric tons and $C_r$ is the unit cost of the rigid beam-to-column connection. In accordance with [11] and [16] the value for the ratio of $C_r/C_s$ is specified as 1.5.

*3.3 Design constraints*

In a structural optimization, design constrains provide a means to assess the behavior of the structure based on code requirements. Design constraints can be classified into three types as [24, 25]: serviceability constraints, ultimate strength constraints, and geometric constrains.

*3.3.1 Serviceability constraints*

At the serviceability stage, the behavior of the structure is evaluated against the gravity loads without the presence of any seismic demands. In this regard, the structural frame is modeled in the absence of infill panels and a gravity load analysis is accomplished under the load combination given by ASCE 7-10 [26]. Then, the adequacy of members is recognized according to the LRFD interaction equation of AISC 360-10 [27] as follows:

$$g_{1,i} = \begin{cases} \dfrac{P_u}{\phi_c P_n} + \dfrac{8}{9}\left(\dfrac{M_{ux}}{\phi_b M_{nx}} + \dfrac{M_{uy}}{\phi_b M_{ny}}\right) \le 0 \ \ if\ \dfrac{P_u}{\phi_c P_n} \ge 0.2 \\ \dfrac{P_u}{2\phi_c P_n} + \left(\dfrac{M_{ux}}{\phi_b M_{nx}} + \dfrac{M_{uy}}{\phi_b M_{ny}}\right) \le 0 \ \ if\ \dfrac{P_u}{\phi_c P_n} < 0.2 \end{cases}, where\ i = 1, \dots, nm \tag{4}$$

where $P_u$ is the required axial strength, $M_u$ is the required moment strength, $P_n$ is the nominal compressive strength, $M_{nx}$ is nominal moment strength about the strong-axis, $M_{ny}$ is nominal moment strength about the weak-axis, $\phi_c$ is the resistance factor for compression and $\phi_b$ is the resistance factor for bending.

*3.3.2 Ultimate strength constraints*

According to ASCE-41 [20], columns are members that are exposed to axial loads greater than 10% of their corresponding axial strength and the other members are identified as beams. The axial compressive load of a column should be considered as a force-controlled action. This constraint can be expressed as follows:

$$g_{2,i}^{j} = \frac{P_{cu,i}^{j}}{P_{c,i}^{j}} - 1 \leq 0 \qquad ,where\ i = 1, \dots, nc\ \ \&\ \ j = LS; CP \tag{5}$$

where $P_{cu,i}^{j}$ is the compressive axial force in member $i$ at the target displacement associated with the $j$th performance level, $P_{c,i}^{j}$ is the available compression strength of member $i$ in connection with performance level $j$ and $nc$ is the number of columns.

The flexural action for all beams and only columns having axial loads less than 50% of their axial compressive strength ($P_c$) needs to be regarded as deformation controlled action. Moreover, flexural load response of columns with axial load value beyond 50% of $P_c$ should be considered as force-controlled action [20]. This constrain can be summarized as follows:

$$g_{3,i}^{j} = \begin{cases} \dfrac{\theta_i^j}{\theta_{all,i}^{j}} - 1 \leq 0 & if\ \ 0 < P_{cu,i}^{j} < 0.5\, P_{c,i}^{j} \\ \dfrac{P_{u,i}^{j}}{P_{c,i}^{j}} + \dfrac{M_{ux,i}^{j}}{M_{cx,i}^{j}} + \dfrac{M_{uy,i}^{j}}{M_{cy,i}^{j}} - 1 \leq 0 & if\ P_{cu,i}^{j} \geq 0.5\, P_{c,i}^{j} \end{cases} \qquad ,where\ i = 1, \dots, nm\ \&\ j = LS; CP \tag{6}$$

where $\theta_i^j$ represents the value of plastic hinge rotation of member $i$ regarding the performance level $j$, $\theta_{max,i}^{j}$ is the allowable plastic hinge rotation of member $i$ for the performance level $j$, $M_{ux,i}$ and $M_{uy,i}$ are the flexural loads of the $i$th member about the strong-axis and weak-axis, respectively, $M_{cx,i}^{j}$ and $M_{cy,i}^{j}$ are respectively available flexural capacities of the member $i$ for the x-axis and y-axis.

Here, the latest ultimate strength constraint is related to the performance of web plates under seismic events. The diagonal tension field in the web plate operates as a deformation-controlled action and its corresponding constraint can be expressed as follows:

$$g_{4,i}^{j} = \frac{\delta_{max,i}^{j}}{\delta_{all,i}^{j}} - 1 \leq 0 \qquad ,where\ \ i = 1, \dots, np \quad \& \quad j = LS; CP \tag{7}$$

where $\delta^{j}_{max\,,i}$ indicates the maximum deformation of the $i$th infill panel at the $j$th performance level and $\delta^{j}_{all\,,i}$ is the allowable deformation of that infill panel.

*3.3.3 Geometric constrains*

For the beam-to-column connection, the flange width of the beam ($b^{b}_{f}$) should not be larger than the flange width of the column ($b^{c}_{f}$). This type of constraint can be stated as follows [16]:

$$g_{5,i} = \frac{b^{b}_{f}}{b^{c}_{f}} - 1.0 \leq 0 \qquad ,where \quad i = l, \dots, nbc \tag{8}$$

where $nbc$ is the number of beam-to-column connections.

*3.4. Constraint handling approach*

In this study, a penalty function method is applied to cope with such a constrained optimization problem. This approach converts the constrained optimization problem into an unconstrained one so that for each violated constraint, the objective function receives a penalty. The penalized objective function $Z(X)$ can be expressed as follows [28]:

$$Z(X) = f_{cost}\,(X) \times f_{penalty}\,(X) = f_{cost}\,(X) \times \left(1 + \varepsilon_1 . \sum_{i=1}^{q} max\,(0, g_i(X))\right)^{\varepsilon_2} \tag{9}$$

where $f_{penalty}\,(X)$ is the penalty function, $g_i(X)$ is the $i$th constraint, $\varepsilon_1$ and $\varepsilon_2$ are two parameters selected based on the exploration and the exploitation rate of the design space, and $q$ is the total number of constraints.

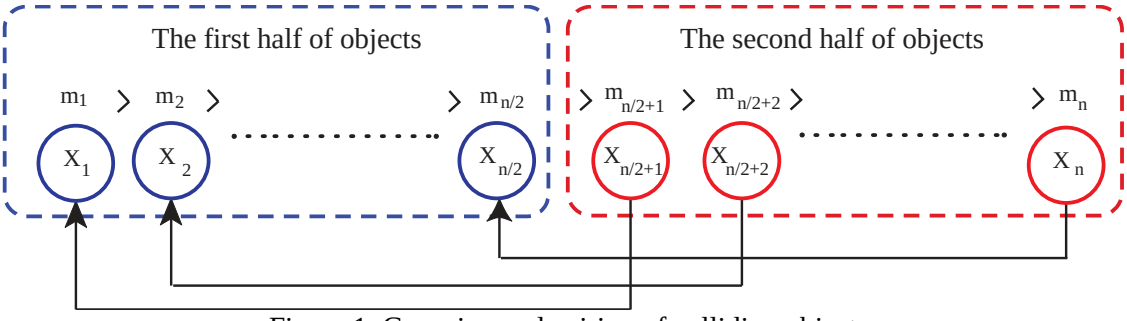


Figure 1. Grouping and pairing of colliding objects

## 4. A HYBRID CBO-JAYA ALGORITHM

This section introduces a new hybrid CBO-Jaya algorithm. More detailed information about the CBO and Jaya algorithms can be found in [17] and [19], respectively. According to the

mechanism of these algorithms, it can be expressed that the both of the algorithms have somewhat the same line of thinking but at different levels. The search strategy of the both algorithm for the movement of each agent can be summarized as: (i) selecting the search direction and (ii) choosing the length of the movement at that direction. Indeed, both algorithms use the position of a bad solution beside from the position of a good one to construct the necessary information for the movement direction. However, in the CBO algorithm, the interaction mechanism takes place at the level of a better/worse solution while in the Jaya algorithm it takes place at the level of the best/worst solution. Also, the length of movement in both of algorithm is selected in a random way. Hence, it could be speculated that CBO and Jaya algorithms provide complementary information, which may enable the CBO-Jaya algorithm to reach the global optimum in a fast and reliable manner. In the CBO-Jaya algorithm, the concepts of moving toward the best solution and getting away from the worst solution are separately considered as an additional velocity for the colliding body before and after the collision in a random manner. Moreover the mechanism of saving the best so-far solutions is adopted from the Jaya algorithm. The overall procedure of the CBO-Jaya algorithm is presented in detail as follows:

Level 1: Initialization

Step 1: The CBO-Jaya algorithm contains a population of colliding bodies, which each of them has a specific position vector. In this stage a random position chosen from the search space is assigned to each colliding body as follows:

$$x_{i,j}^{(0)} = x_{j,min} + rand.\left(x_{j,max} - x_{j,min}\right) \tag{10}$$

where $x_{i,j}^{(0)}$ represents the initial value of the $j$th element (design variable) of the $i$th colliding body position vector (solution vector), $i = 1,2,\dots,n$, $j = 1,2,\dots,D$, $n$ is the number of colliding bodies, D is the size of the search space, $x_{j,min}$ and $x_{j,max}$ are lower and upper bounds of the $j$the design variable, respectively, and $rand$ is a random number uniformly distributed within the range $(0,1)$.

Level 2: Search

Step 1: Each CB is measured regarding the value of its mass as follows [17]:

$$m_i = \frac{1/fit_i}{\sum_{l=1}^{n} 1/fit_i}, \tag{11}$$

where $fit$ represents the objective function value of the solution.

Step 2: The CBs are sorted from best to worst with regard to their amount of mass and then they are split up into two groups having identical number of agents. The collision happens between any members of the two groups having the same rank according to Fig. 1.

Step 3: The physical contact between any two colliding bodies occurs at the position of the first group agent (in line with the CBO algorithm). Apart from that, in this hybrid algorithm it is assumed that each object of the two groups has a tendency of moving toward the best solution or getting away from the worst one in a random manner. At this stage, a random number $\lambda$ which is uniformly distributed within the interval $[0,1]$ is generated. The velocities of the first group objects before the collision can be stated as follows:

$$v_{i,j}^{k} = \begin{cases} -r_{i,j}^{k}.\left(x_{worst\ ,j}^{k} - \left|x_{i,j}^{k}\right|\right) & if\ \lambda > 0.5 \\ +r_{i,j}^{k}.\left(x_{best\ ,j}^{k} - \left|x_{i,j}^{k}\right|\right) & if\ \lambda \le 0.5 \end{cases}, \qquad where\ i = 1,2,\dots,\frac{n}{2} \tag{12}$$

and, for the colliding bodies in the second group, their resultant velocities before the collision must be taken into account as follows:

$$v_{i,j}^{k} = \begin{cases} x_{\left(i-\frac{n}{2}\right),j}^{k} - x_{i,j}^{k} - r_{i,j}^{k}.\left(x_{worst\ ,j}^{k} - \left|x_{i,j}^{k}\right|\right) & if\ \lambda > 0.5 \\ x_{\left(i-\frac{n}{2}\right),j}^{k} - x_{i,j}^{k} + r_{i,j}^{k}.\left(x_{best\ ,j}^{k} - \left|x_{i,j}^{k}\right|\right) & if\ \lambda \le 0.5 \end{cases}, \quad where\ i = \frac{n}{2}+1,\frac{n}{2}+2,\dots,n \tag{13}$$

in which $v_{i,j}^{k}$ represents the value of the $j$th component of the $i$th CB's velocity vector before the collision during the $k$th iteration, $r_{i,j}^{k}$ is a random number in the interval [0,1], which is assigned for the $j$th variable of the $i$th CB in the $k$th iteration, $x_{best\ ,j}^{k}$ and $x_{worst\ ,j}^{k}$ are the values of the $j$th variables for the best and worst agents in the $k$th iteration, respectively and $x_{i,j}^{k}$ is the value of the variable $j$ for the $i$th CB during the $k$th iteration.

Step 4: The CBs are measured for the magnitude of their velocity after the collision. For this purpose, the general form of the equation of velocity after the collision given in [17] is employed as follows:

$$v_{i,j}^{'k} = \begin{cases} \dfrac{\left(m_i^k - \varepsilon m_{(i+\frac{n}{2})}^{k}\right)v_{i,j}^{'k} + (m_{(i+\frac{n}{2})}^{k} + \varepsilon m_{(i+\frac{n}{2})}^{k})v_{\left(i+\frac{n}{2}\right),j}^{'k}}{m_i^k + m_{(i+\frac{n}{2})}^{k}}, & i = 1,\dots,\dfrac{n}{2} \\ \dfrac{\left(m_i^k - \varepsilon m_{(i-\frac{n}{2})}^{k}\right)v_{i,j}^{'k} + (m_{(i-\frac{n}{2})}^{k} + \varepsilon m_{(i-\frac{n}{2})}^{k})v_{\left(i-\frac{n}{2}\right),j}^{'k}}{m_i^k + m_{(i+\frac{n}{2})}^{k}}, & i = \dfrac{n}{2}+1,\dots,n \end{cases} \tag{14}$$

where $v_{i,j}^{'k}$ corresponds to the value of the $j$th element of the velocity vector of the $i$th CB after the collision in the $k$th iteration and $\varepsilon$ is defined in accordance with CBO algorithm [17].

Step 5: Now, CBs that traced the best solution before the collision, move away from the worst solution and vice versa CBs that avoided the worst solution before the collision, move toward the best position. Considering the resultant displacement vector of the CBs, the new position of the first group is determined as:

$$x_{i,j}^{new\ ,k} = \begin{cases} x_{i,j}^{k} + r_{1,i,j}^{k}.v_{i,j}^{'k} + r_{2,i,j}^{k}\left(x_{best\ ,j}^{k} - \left|x_{i,j}^{k}\right|\right) & if\ \lambda > 0.5 \\ x_{i,j}^{k} + r_{1,i,j}^{k}.v_{i,j}^{'k} - r_{2,i,j}^{k}\left(x_{worst\ ,j}^{k} - \left|x_{i,j}^{k}\right|\right) & if\ \lambda \le 0.5 \end{cases} \qquad i = 1,2,\dots,\frac{n}{2} \tag{15}$$

similarly, the new position of the second group is expressed as follows:

$$x_{i,j}^{new,k} = \begin{cases} x_{\left(i-\frac{n}{2}\right),j}^{k} + r_{1,i,j}^{k}.v_{i,j}^{'k} + r_{2,i,j}^{k}\left(x_{best,j}^{k} - \left|x_{i,j}^{k}\right|\right) & if\ \lambda > 0.5 \\ x_{\left(i-\frac{n}{2}\right),j}^{k} + r_{1,i,j}^{k}.v_{i,j}^{'k} - r_{2,i,j}^{k}\left(x_{worst,j}^{k} - \left|x_{i,j}^{k}\right|\right) & if\ \lambda \le 0.5 \end{cases} \quad i = \frac{n}{2}+1, \frac{n}{2}+2, \dots, n \tag{16}$$

where $r_{1,i,j}^{k}$ and $r_{2,i,j}^{k}$ are two random numbers uniformly distributed within the range $(0,1)$.

Step 6: Based on the results obtained from the previous step, if each component for the new position vector of a CB represents that the particle exceeds from its allowable range, it should be adjusted to the nearest lower or upper bound value.

Step 7: At this stage, an assessment is performed on each CB so that if the fitness function value of its new position, $fit(x_{i,j}^{new,k})$, surpasses the fitness function value of its current position, $fit(x_{i,j}^{k})$, the new solution is appointed for the attendance in the next iteration, otherwise the current solution participates in the next iteration without any change. This description can be summarized as follows:

$$x_{i,j}^{k+1} = \begin{cases} x_{i,j}^{new,k} & fit(x_{i,j}^{new,k}) > fit(x_{i,j}^{k}) \\ x_{i,j}^{k} & otherwise \end{cases}, \qquad i = 1,2,\dots,n \tag{17}$$

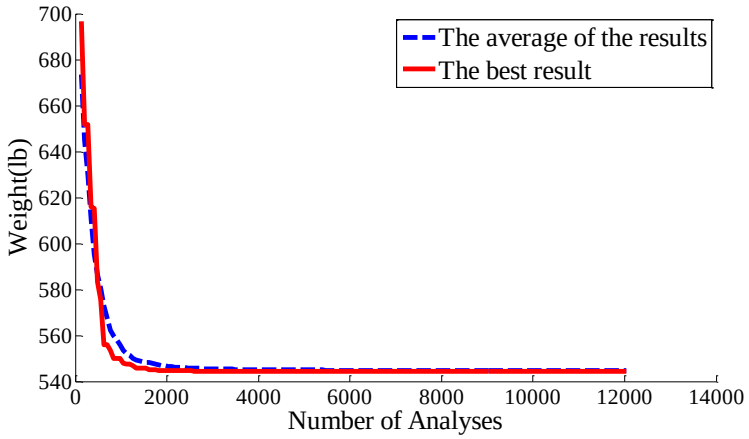


Figure 2. The convergence curve for the 25-bar spatial truss

## 5. APPLICATION OF THE CBO-JAYA ALGORITHM TO THE TEST PROBLEMS

In order to validate the efficiency and applicability of the proposed hybrid algorithm, two common benchmark optimization problems are investigated. The results of the CBO-Jaya algorithm are compared with the CBO algorithm and other meta-heuristic algorithms from the literature. In all of the examples, initial population size was set to be 70 for the proposed hybrid algorithm. Due to the random nature of the meta-heuristic algorithms 20 independent

runs were carried out to provide a significant outcome. The maximum number of function evaluations of 12,000 and 16,000 was applied as the convergence criteria for these two examples, respectively. A penalty function method was utilized to handle the constraints. The optimization algorithm and the required structural analysis were implemented using MATLAB.

Table 1: Comparison of the optimum designs for the 25-bar spatial truss

| Element group | Optimal cross-sectional areas ($in.^2$) | | | | |
|---|---|---|---|---|---|
| | Schutte and Groenwold PSO [29] | Lee and Geem HS [30] | Kaveh and Khayatazad RO [31] | Kaveh and Mahdavi CBO [28] | Present work |
| 1 | 0.010 | 0.047 | 0.0157 | 0.0100 | 0.0100 |
| 2-5 | 2.121 | 2.022 | 2.0217 | 2.1297 | 1.9653 |
| 6-9 | 2.893 | 2.95 | 2.9319 | 2.8865 | 2.9861 |
| 10-11 | 0.010 | 0.010 | 0.0102 | 0.0100 | 0.0100 |
| 12-13 | 0.010 | 0.014 | 0.0109 | 0.0100 | 0.0100 |
| 14-17 | 0.671 | 0.688 | 0.6563 | 0.6792 | 0.6936 |
| 18-21 | 1.611 | 1.657 | 1.6793 | 1.6077 | 1.6797 |
| 22-25 | 2.717 | 2.663 | 2.7163 | 2.6927 | 2.6550 |
| Best weight (lb) | 545.21 | 544.38 | 544.656 | 544.310 | 544.2329 |
| Average weight (lb) | 546.84 | N/A | 546.689 | 545.256 | 544.5451 |
| Standard deviation | 1.478 | N/A | 1.612 | 0.294 | 0.3649 |
| Number of analyses | 9,596 | 15,000 | 13,880 | 9,090 | 7,770 |

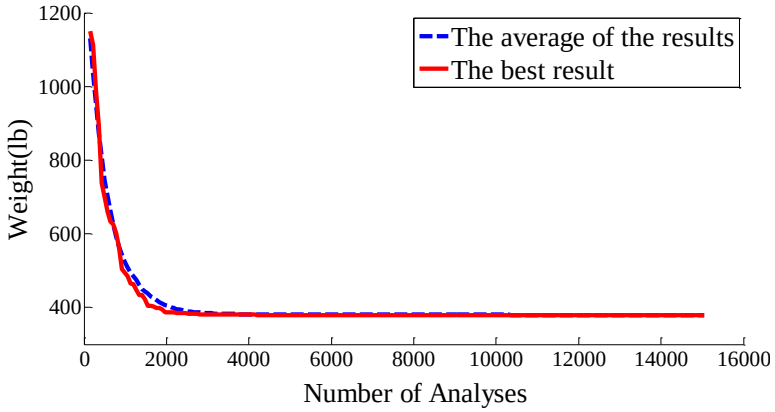


Figure 3. The convergence curve for the 72-bar spatial truss

*5.1. A 25-Bar spatial truss*

A 25-bar spatial truss structure has been widely employed in literature to examine the performance of the optimization algorithms. The aim of this problem is to minimize the weight of the truss structure subject to displacement and stress constraints. More details about the problem can be found in [28]. Table 1 compares the optimum results obtained by the CBO-Jaya algorithm and other meta-heuristic algorithms for the 25-bar spatial truss problem. As shown, the CBO-Jaya algorithm achieved the best solution of 544.233lb, which

is slightly better than others. Also, the proposed algorithm has the mean result of 544.545lb, which is the best among those reported in literature. The best solution provided by the CBO-Jaya algorithm relies on approximately 7,770 analyses, which is much less than other methods. As detailed in Table 1, the standard deviation of the CBO-Jaya algorithm with the value of 0.326 stands in the second place among the available researches. The convergence history of the CBO-Jaya algorithm for this problem is shown in Fig. 2. It is apparent from the figure that the proposed algorithm has high convergence ability to the best solution. The CBO-Jaya algorithm could achieve the best solution obtained by the CBO algorithm only in approximately 3,220 analyses, which represents a 65% reduction in computational effort at this level.

Table 2: Comparison of the optimum designs for the 72-bar spatial truss

| Element group | Optimal cross-sectional areas ($in.^2$) | | | | | |
|---|---|---|---|---|---|---|
| | Camp and Bichon ACO [32] | Perez and Behdinan PSO [33] | Camp BB-BC [34] | Kaveh and Khayatazad RO [31] | Kaveh and Mahdavi CBO [28] | Present work |
| 1-4 | 1.948 | 1.7427 | 1.8577 | 1.8365 | 1.9028 | 1.8762 |
| 5-12 | 0.508 | 0.5185 | 0.5059 | 0.5021 | 0.518 | 0.5096 |
| 13-16 | 0.101 | 0.1 | 0.1 | 0.1 | 0.1001 | 0.1 |
| 17-18 | 0.102 | 0.1 | 0.1 | 0.1004 | 0.1003 | 0.1 |
| 19-22 | 1.303 | 1.3079 | 1.2476 | 1.2522 | 1.2787 | 1.2702 |
| 23-30 | 0.511 | 0.5193 | 0.5269 | 0.5033 | 0.5074 | 0.5119 |
| 31-34 | 0.101 | 0.1 | 0.1 | 0.1002 | 0.1003 | 0.1 |
| 35-36 | 0.100 | 0.1 | 0.1012 | 0.1001 | 0.1003 | 0.1 |
| 37-40 | 0.561 | 0.5142 | 0.5209 | 0.573 | 0.524 | 0.537 |
| 41-48 | 0.492 | 0.5464 | 0.5172 | 0.5499 | 0.515 | 0.5151 |
| 49-52 | 0.1 | 0.1 | 0.1004 | 0.1004 | 0.1002 | 0.1 |
| 53-54 | 0.107 | 0.1095 | 0.1005 | 0.1001 | 0.1015 | 0.1 |
| 55-58 | 0.156 | 0.1615 | 0.1565 | 0.1576 | 0.1564 | 0.1562 |
| 59-66 | 0.550 | 0.5092 | 0.5507 | 0.5222 | 0.5494 | 0.548 |
| 67-70 | 0.390 | 0.4967 | 0.3922 | 0.4356 | 0.4029 | 0.4123 |
| 71-72 | 0.592 | 0.5619 | 0.5922 | 0.5971 | 0.5504 | 0.5707 |
| Best weight (lb) | 380.24 | 381.91 | 379.85 | 380.458 | 379.6943 | 379.6277 |
| Average weight (lb) | 383.16 | N/A | 382.08 | 382.553 | 379.8961 | 379.6806 |
| Standard deviation | 3.66 | N/A | 1.912 | 1.221 | 0.0791 | 0.0568 |
| Number of analyses | 18,500 | N/A | 19,621 | 19,084 | 15,600 | 11,970 |

*5.2 A 72-bar spatial truss structure*

A detailed description of this problem can be found in [28]. The optimization results of the CBO-Jaya algorithm and other meta-heuristic algorithms for the 72-bar spatial truss are summarized in Table 2. The optimum solution found by the CBO-Jaya algorithm is

379.6342 lb, which is the best solution overall. Also, the average result and the standard deviation of 20 independent runs gained for the proposed algorithm appear to be the best among other algorithms. The CBO-Jaya algorithm requires approximately 11,970 analyses to attain the optimum result, which is noticeably less that other method. The convergence history of the CBO-Jaya algorithm for the 72-bar spatial truss is given in Fig. 3. Once again, the high convergence ability of the proposed algorithm to the best solution can be observed. The CBO-Jaya algorithm could achieve a solution weighted by 380 lb after approximately 3,549 analyses, which is equivalent to 99% of the final solution.

The results of the benchmark problems demonstrate the accuracy, reliability and speed of convergence of the CBO-Jaya algorithm to obtain the optimum solution.

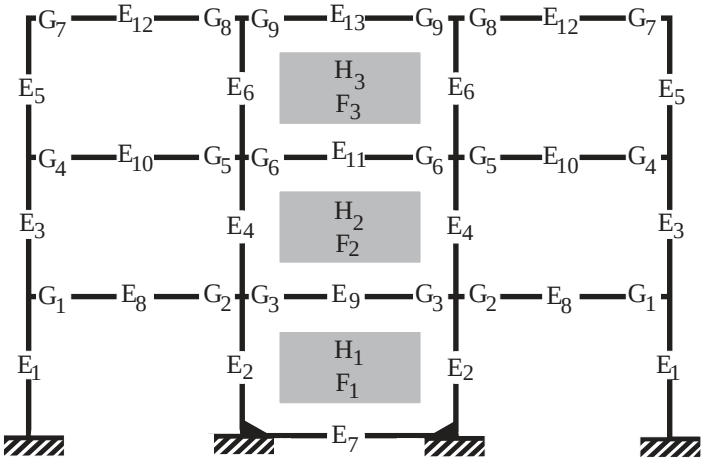


Figure 4. Design group numbers for $SPSW_I$

## 6. OPTIMIZATION OF THE SPSW ANALYTICAL MODEL

A three-story, three-bay steel frame with typical bay width of 6.10 m (20 ft) and the typical story height of 3.96 m (13 ft) in which infill panels are placed in its middle bay is adopted as the basic model of the present investigation. The general characteristics of the model such as material properties, dead loads, live loads, the seismic mass, and the type of site class for the seismic design are assumed to be consistent with the SPSW3W model developed by Berman [23]. For comparison purposes, the optimization task is performed for the following three cases:

- $SPSW_I$: The size of components and the arrangement of connections for the SPSW model are simultaneously optimized.
- $SPSW_{II}$: The size of components for the SPSW model with conventional connection arrangement is optimized.
- $SPSW_{III}$: The size of components for the SPSW model with the connection arrangement proposed by Xue and Lu [4] is optimized.

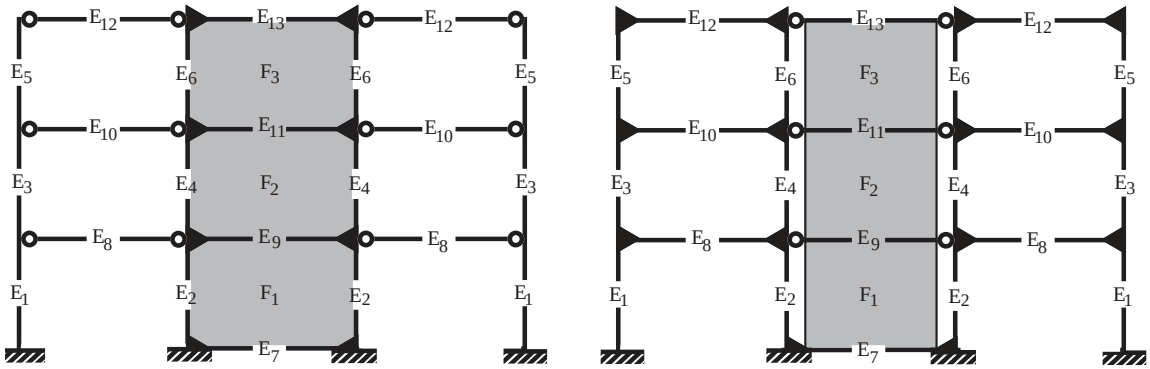


(a) (b)

Figure 5. Connection arrangement and design group numbers for: (a) $SPSW_{II}$ and (b) $SPSW_{III}$

Fig. 4 shows assigned design group numbers for $SPSW_I$ and Fig. 5 indicates the configuration as well as beam, column, and infill panel group numbers for $SPSW_{II}$ and $SPSW_{III}$. In these cases, beams are selected from all 267 W-shaped sections and columns are chosen from W14 and W12 sections. For infill panels, ASTM A36 plate thicknesses tabulated in [9] are chosen. In order to simulate the behavior of the fully-connected infill panels and the beam-only-connected infill panels, a standard strip model [9] and a partial tension field strip model [35, 36] are employed, respectively. Based on the strip model, solid web plates are substituted by a serious of tension-only, pin-ended elements that are equally spaced along the direction of the tension field. For the standard strip model, the deviation angle of the tension strip relative to the vertical direction is affected by the dimensions of the web plate and the cross sectional properties of its surrounding elements, however this angle can be adjusted to an average value [37]. The deviation angle of the partial tension field relative to the vertical direction, $\theta$, only depends on the geometry of the infill panel, which can be calculated as follows [35,36]:

$$tan(2\theta) = \frac{L}{h} \tag{18}$$

where $L$ is the bay width and $h$ is the typical story height.

In the present study, the infill panels must be modeled in such a way that they have the potential to capture either the fully-connected infill panel or beam-only-connected infill panel at the same time during the optimization procedure. Moreover, this model should prevent the appearance of staggered points at the HBEs as described in [9]. Hence, after some trial and error 17 fully-connected strips having the inclination angle of $44^{\circ}$ with respect to the vertical direction and 8 beam-only-connected strip having the inclination angle of $29^{\circ}$ with vertical were selected to model the infill panels as shown in Fig. 6. In this paper, OpenSees [38] is utilized to perform all required analyses including the gravity analysis, linear dynamic analysis and pushover analysis.

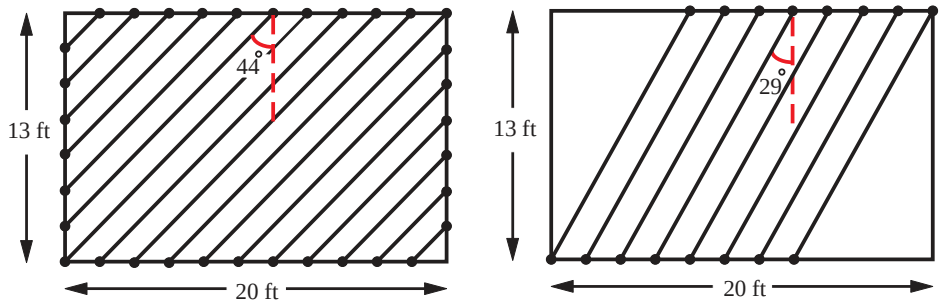


(a) Fully-connected infill panel (b) Partially-connected infill panel

Figure 6. Strip models utilized in the present study

All strips are modeled using the *Truss Element*s of OpenSees [38] whose material models are defined as the *Hysteretic Uniaxial Material* model and *Elastic Material* model for the nonlinear pushover analysis and the elastic analyses, respectively. The frame members for the nonlinear pushover analysis are modeled by employing *nonlinear Beam Column* force-based element in OpenSees [38] to consider the distributed plasticity along the frame members. Furthermore, fiber sections with 16 fibers along the flange width and 33 fibers along the web depth and *Hysteretic Uniaxial Material* model are appointed to represent the interaction behavior between the axial forces and flexural moments at frame members. One common problem with the use of nonlinear static pushover analysis during the optimization procedure is that the convergence may not be achieved. Hence, the script specified in the OpenSees Command Language Manual [38] for this purpose, which inevitably increases the computation time is added to the main pushover analysis commands. The CBO-Jaya optimization algorithm that its efficiency was demonstrated in previous section is utilized to optimize the three SPSW cases. The population size is taken as 70 and the maximum number of structural analyses is set to 10,000 as the termination criterion for the CBO-Jaya algorithm. Due to the considerably time-consuming nature of the problem, a single run is carried out. The optimization algorithm is coded in MATLAB. During the optimization procedure, MATLAB and OpenSees [38] are linked together. The programs are executed on a personal computer with Intel Core i7 CPU 4.0 GHz and 16GB of RAM.

## 7. RESULTS AND DISCUSSION

### *7.1 Costs*

The optimal results obtained for the three SPSW cases are reported in Table 3. The CBO-Jaya algorithm achieved a design for $SPSW_I$ with minimum cost of 27.86 metric tons, which is 23% and 33% less than the minimum total costs of 36.18 and 41.91 metric tons obtained for $SPSW_{II}$ and $SPSW_{III}$, respectively. The arrangement of connections for the optimal solution of $SPSW_I$ is shown in Fig. 7. As it is depicted, the location of rigid beam-to-column connections is limited only to the middle bay of the first floor level. Moreover, both types of the fully-connected web plate and the beam-only-connected web plate can be observed in

such a design. It should be noted that due to the random nature of the algorithm, this configuration is not unique and different optimal configuration may be achieved by performing re-optimization.



Table 3: Optimal designs for the three SPSW cases

| Design group | SPSW ID | | |
|---|---|---|---|
| | $SPSW_I$ | $SPSW_{II}$ | $SPSW_{III}$ |
| $E_1$ | W12×22 | W14×26 | W12×96 |
| $E_2$ | W14×605 | W14×730 | W14×426 |
| $E_3$ | W14×26 | W12×16 | W12×190 |
| $E_4$ | W14×311 | W14×311 | W14×120 |
| $E_5$ | W14×22 | W12×16 | W14×43 |
| $E_6$ | W14×176 | W14×109 | W14×120 |
| $E_7$ | W21×62 | W36×441 | W24×162 |
| $E_8$ | W12×30 | W16×40 | W21×132 |
| $E_9$ | W24×229 | W14×132 | W36×135 |
| $E_{10}$ | W14×48 | W21×73 | W24×117 |
| $E_{11}$ | W36×135 | W18×143 | W27×114 |
| $E_{12}$ | W30×99 | W27×102 | W18×106 |
| $E_{13}$ | W36×262 | W24×131 | W30×108 |
| $F_1$ | 1.71 mm | 1.90 mm | 1.59 mm |
| $F_2$ | 4.76 mm | 3.18 mm | 2.66 mm |
| $F_3$ | 3.18 mm | 2.66 mm | 1.90 mm |
| $G_1$ | S* | - | - |
| $G_2$ | S | - | - |
| $G_3$ | R | - | - |
| $G_4$ | S | - | - |
| $G_5$ | S | - | - |
| $G_6$ | S | - | - |
| $G_7$ | S | - | - |
| $G_8$ | S | - | - |
| $G_9$ | S | - | - |
| $H_1$ | P | - | - |
| $H_2$ | P | - | - |
| $H_3$ | F | - | - |
| Cost in metric tons | 27.862 | 36.179 | 41.908 |
| CPU time (hr) | 112 | 121 | 105 |

*S: Simple beam-to-column connection; R: Rigid beam-to-column connection; P: Partially-connected infill panel; F: Fully-connected infill panel

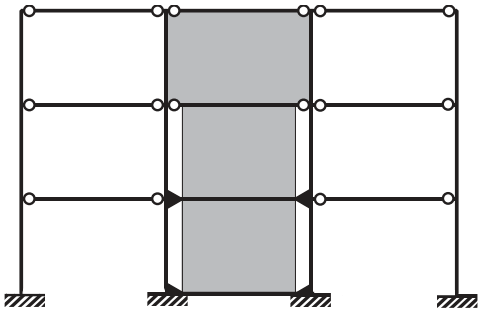

Figure 7. Optimal connection arrangement obtained for $SPSW_I$

The contributions of structural components and rigid connections of the optimized SPSWs to their total cost are compared in Fig. 8 and the corresponding values are presented in Table 4. It is apparent from the results that the connection cost could have a considerable impact on the total cost while infill panel comprises a small portion of that. The optimal solution of $SPSW_I$ involves a good balance between the cost of its parts so that it stands in the first, second and third place with regard to the cost of connections, frame members and infill panels, respectively. The heaviest frame members belong to $SPSW_{II}$ as was predictable for such as SPSW with conventional configuration. Without considering the connection cost, $SPSW_{III}$ has the best weight among the others, which is in agreement with the results of Xue and Lu [4], however when comparing the overall cost, it drops to the third place.

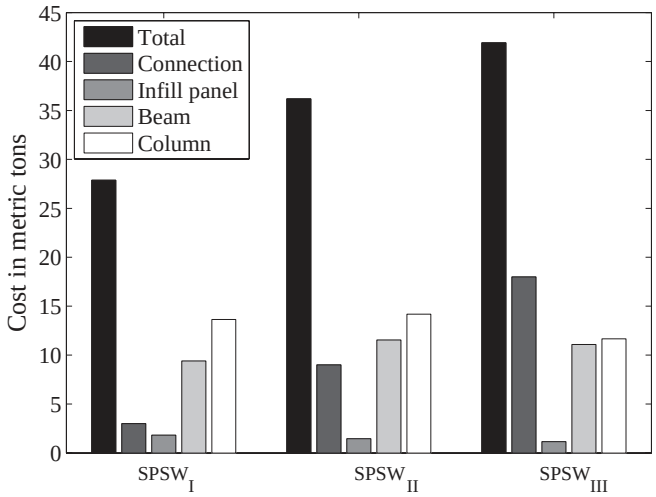


Figure 8. Comparison of material and connection costs for three SPSW cases

Table 4: Detailed values of the material and connection costs for three SPSW cases

| SPSW ID | Costs in metric tons | | | | |
|---|---|---|---|---|---|
| | Total | Connection | Infill panel | Beam | Column |
| $SPSW_I$ | 27.862 | 3 | 1.819 | 9.399 | 13.643 |
| $SPSW_{II}$ | 36.179 | 9 | 1.457 | 11.533 | 14.188 |
| $SPSW_{III}$ | 41.908 | 18 | 1.158 | 11.088 | 11.661 |

The results of the cost comparison demonstrate that simultaneous optimization of size and connection arrangement for the SPSW model could result in a considerable reduction in the overall cost compared to those obtained by pure sizing optimization. In this way, the optimization algorithm aims to minimize the overall cost of the SPSW by achieving the best trade-off between the costs of components and connections.

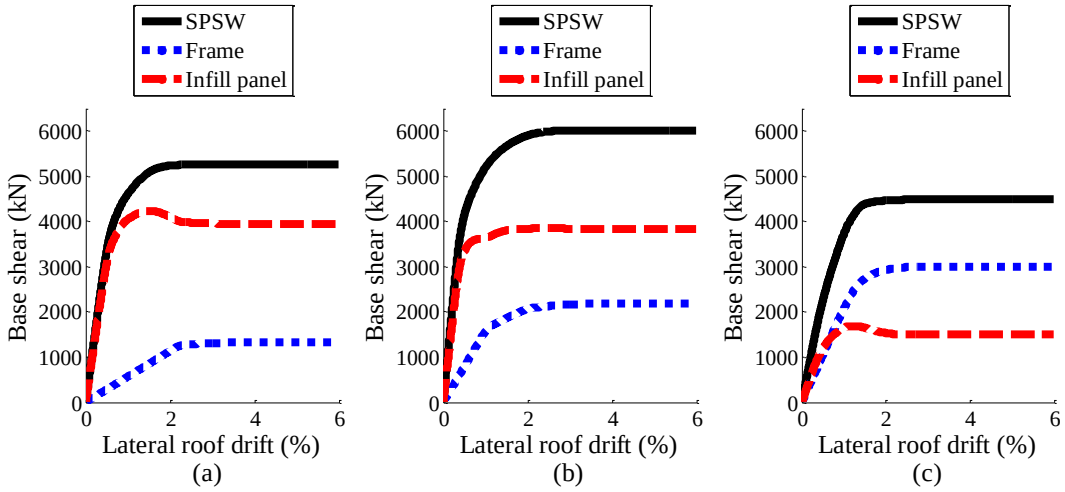


Figure 9. Pushover capacity curves for: (a) $SPSW_I$; (b) $SPSW_{II}$ and (c) $SPSW_{III}$

*7.2 Strength and stiffness*

The pushover curves of the three optimized SPSWs and the contributions of their web plate and frame member components to the total capacity are given in Fig. 9. The force-displacement relationship of the infill panel component for each optimized frame is obtained by subtracting the pushover curve of the frame member component from the pushover curve of the entire structure. The numerical values of the ultimate base shear strength and the over-strength factor (ratio of the ultimate-to-design base shear strength) for the three SPSW cases are also summarized in Table 5. As can be seen in Table 5, the ultimate base shear strength of $SPSW_I$, $SPSW_{II}$, and $SPSW_{III}$ are 5268.9, 6014.9, and 4493.6 kN, respectively. It is evident that these values are almost close to each other, however $SPSW_{III}$ exhibits slightly lower strength compared to other cases. Moreover, the percentages of base shear resisted by the infill panels are 75%, 64% and 33% for $SPSW_I$, $SPSW_{II}$, and $SPSW_{III}$, respectively. Accordingly, it can be inferred that a more optimal design for a SPSW can be obtained by reducing the portion of base shear resisted by the frame members and increasing the portion of infill panels to compensate the lack of load-carrying capacity.

As shown in Table 5 the over-strength factors for the cases of $SPSW_I$, $SPSW_{II}$, and $SPSW_{III}$ are 2.4, 2.7, and 2.0, respectively. This implies that having such a high over-strength factor may be necessary even for an optimized SPSW. This result is in agreement with the Purba and Bruneau [39] who demonstrated that eliminating the SPSW over-strength leads to a design that does not meet the required seismic performance.

Table 5: Ultimate base shear strength, design base shear and over-strength factor for the optimized SPSWs

| SPSW ID | Ultimate base shear strength (kN) | | | $\frac{V_P}{V}$ (%) | $\frac{V_F}{V}$ (%) | Design base shear (kN) | Over-strength factor ($\Omega_0$) |
|---|---|---|---|---|---|---|---|
| | Total ($V$) | Infill panel ($V_P$) | Frame ($V_F$) | | | | |
| $SPSW_I$ | 5268.9 | 3948.7 | 1320.2 | 75 | 25 | 2206.3 | 2.4 |
| $SPSW_{II}$ | 6014.9 | 3838.4 | 2176.5 | 64 | 36 | 2206.3 | 2.7 |
| $SPSW_{III}$ | 4493.6 | 1495.1 | 2998.5 | 33 | 67 | 2206.3 | 2.0 |

The initial stiffness, target displacement at LS and CP performance levels, and the elastic fundamental period of the structure for the three optimized SPSW are summarized in Table 6. As shown, $SPSW_{II}$ has the highest initial stiffness (lowest elastic fundamental period), $SPSW_{III}$ contains the lowest initial stiffness (highest elastic fundamental period), and $SPSW_I$ is rated as second place with this regard. It seems that the use of partial infill panel connections has a negative impact on initial stiffness of the SPSW. However, the appropriate use of beam-only-connected infill panels in conjunction with the fully-connected-infill panels along the height of the story, similar to that obtained for $SPSW_I$, could lead to a good design.

Table 6: Initial stiffness, target displacement, and period for the optimized frames

| SPSW ID | Initial stiffness (kN/mm) | | | Target displacement (mm) | | Period (s) |
|---|---|---|---|---|---|---|
| | Total | Infill panel | Frame | LS | CP | |
| $SPSW_I$ | 68.14 | 63.04 | 5.096 | 287.7 | 538.4 | 0.772 |
| $SPSW_{II}$ | 91.31 | 75.60 | 15.71 | 248.6 | 467.1 | 0.656 |
| $SPSW_{III}$ | 45.21 | 23.95 | 21.24 | 330.7 | 612.39 | 0.930 |

## 8. CONCLUSIONS

Conventional configuration of SPSW system results in an uneconomical design. In this paper, simultaneous optimization of size and connection arrangement for low-rise SPSWs is investigated to seek a new way of addressing the mentioned issue. The optimization problem is formulated as a cost minimization problem in which the cross-sectional area of beams and columns, the thickness of infill panels, the type of each beam-to-column connection (either simple or rigid), and the type of each infill-to-boundary frame connection (either full or partial) are regarded as design variables and the objective function is considered as the sum of the material cost and the rigid connection fabrication cost. The assessment of structural behavior is carried out within the framework of performance-based seismic design using nonlinear static pushover analysis. The numerical model contains a three-story, three-bay steel frame, in which infill panels are located in the middle bay. Besides the simultaneous optimization of size and connection arrangement for the model ($SPSW_I$), the pure sizing optimization is performed with regard to the conventional connection arrangement ($SPSW_{II}$)

and that proposed by Xue and Lu [4] ($SPSW_{III}$) as a basis for comparison. In order to tackle the optimization problem, a new hybrid optimization algorithm called CBO-Jaya is proposed. The present hybrid algorithm has almost the main body of the CBO algorithm, in which the strategies of the Jaya algorithm are effectively added to determine the search direction. Firstly, the performance of the proposed algorithm is evaluated on two benchmark optimization problems and then it is applied to optimize the SPSW model. The results obtained for the benchmark problems reveal the ability of the proposed algorithm to achieve better optimum solution in significantly lower number of function evaluations compared to those of attained by other techniques in literature. The optimization of the $SPSW_I$ resulted in a solution with 23% and 33% lower cost compared to those of gained for $SPSW_{II}$ and $SPSW_{III}$, respectively. This result clearly reveals that when the optimal arrangement of the beam-to-column and infill-to-boundary frame connections are participated in the optimization process of a low-rise SPSW, a more cost-effective design can be achieved. Furthermore, from the comparison of the capacity curve attained for the SPSWs, it could be concluded that reducing the base shear strength of frame members and increasing the share of infill panels in compensation is accompanied by a more low-cost design. Further work is needed to deal with the time-consuming nature of the present problem and carry out the optimization procedure in several independent runs to enhance the reliability of the results. Moreover, future work could replicate the present study regarding the high-rise SPSW systems.

## REFERENCES

1. Astaneh-Asl A. Seismic behavior and design of steel plate shear walls, steel technical information and product services report, *Structural Steel Educational Council*, Moraga, California, 2001.
2. Qu B, Bruneau M. Behavior of vertical boundary elements in steel plate shear walls, *Eng J (Chicago)* 2010; **47**(2): 109-22.
3. Berman JW, Lowes LN, Okazaki T, Bruneau M, Tsai KC, Driver RG, Sabelli R, Moore W. Research needs and future directions for steel plate shear walls, *Proceeding of the 2008 Structures Congress* 2008, Vancouver, Canada, pp. 1-10.
4. Xue M, Lu LW. Interaction of infilled steel shear wall panels with surrounding frame members, *Proceedings of the Structural Stability Research Council Annual Technical Session* 1994, Bethlehem, PA, pp. 339-54.
5. Berman JW, Bruneau M. Experimental investigation of light-gauge steel plate shear walls, *J Struct Eng* 2005; **131**(2): 259-67.
6. Chen SJ, Jhang C. Cyclic behavior of low yield point steel shear walls, *Thin wall struct* 2006; **44**(7): 730-8.
7. Li CH, Tsai KC. Experimental responses of four 2-story narrow steel plate shear walls, *Proceeding of the Structures Congress*, Vancouver, Canada, 2008, pp. 1-10.
8. Vian D, Bruneau M, Tsai KC, Lin YC. Special perforated steel plate shear walls with reduced beam section anchor beams. I: Experimental investigation, *J Struct Eng* 2009; **135**(3): 211-20.

9. Sabelli R, Bruneau M. *Design guide 20 Steel Plate Shear Walls*, American Institute of Steel Construction, Chicago, USA, 2007.
10. Choi IR, Park HG. Steel plate shear walls with various infill plate designs, *J Struct Eng* 2009; **135**(7): 785-96.
11. Kripakaran P, Hall B, Gupta A. A genetic algorithm for design of moment-resisting steel frames, *Struct Multidisc Optim* 2011; **44**(4): 559-74.
12. Kaveh A, Farhoudi N. A unified approach to parameter selection in meta-heuristic algorithms for layout optimization, *J Construct Steel Res* 2011; **67**(10): 1453-62.
13. Gholizadeh S, Shahrezaei AM. Optimal placement of steel plate shear walls for steel frames by bat algorithm, *Struct Des Tall Special Build* 2015; **24**(1): 1-8.
14. Kaveh A, Azar BF, Hadidi A, Sorochi FR, Talatahari S. Performance-based seismic design of steel frames using ant colony optimization, *J Construct Steel Res* 2010; **66**(4): 566-74.
15. Kaveh A, Nasrollahi A. Performance-based seismic design of steel frames utilizing charged system search optimization, *Appl Soft Comput* 2014; **22**: 213-21.
16. Alberdi R, Murren P, Khandelwal K. Connection topology optimization of steel moment frames using metaheuristic algorithms, *Eng Struct* 2015; **100**: 276-92.
17. Kaveh A, Mahdavi VR. Colliding bodies optimization: a novel meta-heuristic method, *Comput Struct* 2014; **139**: 18-27.
18. Kaveh A, Mahdavi VR. A hybrid CBO-PSO algorithm for optimal design of truss structures with dynamic constraints, *Appl Soft Comput* 2015; **34**: 260-73.
19. Rao R. Jaya: A simple and new optimization algorithm for solving constrained and unconstrained optimization problems, *Int J Industrial Eng Comput* 2016; **7**(1): 19-34.
20. ASCE/SEI 41-06, *Seismic Rehabilitation of Existing Buildings*, American Society of Civil Engineers, Reston, Virginia, 2007.
21. Kaveh A, Laknejadi K, Alinejad B. Performance-based multi-objective optimization of large steel structures, *Acta Mech* 2012; **223**(2): 355-69.
22. Moghimi H, Driver RG. Column demands in steel plate shear walls with regular perforations using performance-based design methods, *J Construct Steel Res* 2014; **103**: 13-22.
23. Berman JW. Seismic behavior of code designed steel plate shear walls, *Eng Struct* 2011; **33**(1): 230-44.
24. Kaveh A, Bakhshpoori T, Azimi M. Seismic optimal design of 3D steel frames using cuckoo search algorithm, *Structu Des Tall Special Build* 2015; **24**(3): 210-27.
25. Gholizadeh S, Poorhoseini H. Seismic layout optimization of steel braced frames by an improved dolphin echolocation algorithm, *Struct Multidisc Optim* 2016; **54**(4): 1011-29.
26. ASCE/SEI 7-10, *Minimum Design Loads for Buildings and other Structures*, American Society of Civil Engineers, Reston, Virginia, 2010.
27. ANSI/AISC 360-10, *Specification for Structural Steel Buildings*, American Institute of Steel Construction, Chicago, Illinois, 2010.
28. Kaveh A, Mahdavi VR. Colliding bodies optimization method for optimum design of truss structures with continuous variables, *Adv Eng Softw* 2014; **70**: 1-12.
29. Schutte JF, Groenwold AA. Sizing design of truss structures using particle swarms, *Struct Multidisc Optim* 2003; **25**(4): 261-9.

30. Lee KS, Geem ZW. A new structural optimization method based on the harmony search algorithm, *Comput Struct* 2004; **82**(9): 781-98.
31. Kaveh A, Khayatazad M. A new meta-heuristic method: ray optimization, *Comput Struct* 2012; **112**: 283-94.
32. Camp CV, Bichon BJ. Design of space trusses using ant colony optimization, *J Struct Eng* 2004; **130**(5): 741-51.
33. Perez RE, Behdinan K. Particle swarm approach for structural design optimization, *Comput Struct* 2007; **85**(19): 1579-88.
34. Camp CV. Design of space trusses using Big Bang–Big Crunch optimization, *J Struct Eng* 2007; **133**(7): 999-1008.
35. Clayton PM, Berman JW, Lowes LN. Seismic performance of self-centering steel plate shear walls with beam-only-connected web plates, *J Construct Steel Res* 2015; **106**: 198-208.
36. Vatansever C, Yardimci N. Experimental investigation of thin steel plate shear walls with different infill-to-boundary frame connections, *Steel Compos Struct* 2011; **11**(3): 251-71.
37. Qu B, Guo X, Chi H, Pollino M. Probabilistic evaluation of effect of column stiffness on seismic performance of steel plate shear walls, *Eng Struct* 2012; **43**: 169-79.
38. Mazzoni S, McKenna F, Scott MH, Fenves GL. *OpenSees Command Language Manual*, Pacific Earthquake Engineering Research (PEER) Center, Berkeley, California, 2006.
39. Purba R, Bruneau M. Seismic performance of steel plate shear walls considering two different design philosophies of infill plates. II: Assessment of collapse potential, *J Struct Eng* 2014; **141**(6): 04014161.